Structural Framework for Covalent Inhibition of Clostridium botulinum Neurotoxin A by Targeting Cys165.

Enrico A Stura, Laura Le Roux, Karine Guitot, Sandra Garcia, Sarah Bregant, Fabrice Beau, Laura Vera, Guillaume Collet, Denis Ptchelkine, Huseyin Bakirci, et al.

THE JOURNAL OF BIOLOGICAL CHEMISTRY VOL. 287, NO. 40, pp. 33607–33614, September 28, 2012

Structural Framework for Covalent Inhibition of *Clostridium botulinum* Neurotoxin A by Targeting Cys^{165}*[S]

Received for publication, June 29, 2012, and in revised form, August 3, 2012 Published, JBC Papers in Press, August 6, 2012, DOI 10.1074/jbc.M112.396697

Enrico A. Stura, Laura Le Roux, Karine Guitot, Sandra Garcia, Sarah Bregant, Fabrice Beau, Laura Vera, Guillaume Collet, Denis Ptchelkine, Huseyin Bakirci, and Vincent Dive[1]

From the Commissariat à l'Energie Atomique, iBiTec-S, Service d'Ingénierie Moléculaire des Protéines, CE-Saclay, 91191 Gif-sur-Yvette, Cedex, France

Background: Development of small potent synthetic inhibitors of *Clostridium botulinum* neurotoxin A remains an unresolved challenge.
Results: Small compounds incorporating electrophile moiety can block enzyme activity by covalent modification of Cys^{165}.
Conclusion: A structural framework for developing potent covalent inhibitors of *Clostridium botulinum* neurotoxin A is provided.
Significance: This study uncovers a subfamily of zinc proteases containing a conserved cysteine in their active site.

Clostridium botulinum **neurotoxin type A (BoNT/A) is one of the most potent toxins for humans and a major biothreat agent. Despite intense chemical efforts over the past 10 years to develop inhibitors of its catalytic domain (catBoNT/A), highly potent and selective inhibitors are still lacking. Recently, small inhibitors were reported to covalently modify catBoNT/A by targeting Cys^{165}, a residue located in the enzyme active site just above the catalytic zinc ion. However, no direct proof of Cys^{165} modification was reported, and the poor accessibility of this residue in the x-ray structure of catBoNT/A raises concerns about this proposal. To clarify this issue, the functional role of Cys^{165} was first assessed through a combination of site-directed mutagenesis and structural studies. These data suggested that Cys^{165} is more involved in enzyme catalysis rather than in structural property. Then by peptide mass fingerprinting and x-ray crystallography, we demonstrated that a small compound containing a sulfonyl group acts as inhibitor of catBoNT/A through covalent modification of Cys^{165}. The crystal structure of this covalent complex offers a structural framework for developing more potent covalent inhibitors catBoNT/A. Other zinc metalloproteases can be founded in the protein database with a cysteine at a similar location, some expressed by major human pathogens; thus this work should find broader applications for developing covalent inhibitors.**

The anaerobic spore-forming bacteria *Clostridium botulinum* produces the most potent neurotoxins known. These toxins, the causative agents of botulism, impair the release of acetylcholine from presynaptic nerve terminals at neuromuscular junctions through specific proteolysis of essential SNARE proteins (1, 2). The Centers for Disease Control and prevention have classified these toxins in category A of biowarfare agents. Among the seven serotypes of *botulinum* neurotoxins so far described, serotype A (BoNT/A)[2] specifically cleaves the synaptosome-associated 25-kDa protein (SNAP-25) (3). BoNT/A is synthesized as a 150-kDa single polypeptide chain, which is then cleaved by endogenous proteases to give the two chains structure consisting of a 50-kDa light chain linked by a single disulfide bond to a 100-kDa heavy chain. The heavy chain is responsible for specific cell surface receptor interactions, and the light chain is a zinc metalloprotease that cleaves SNAP-25. Disulfide bond reduction is essential for allowing free access of SNAP-25 to the light proteolytic active site (4). Because BoNT/A is the most potent neuron-blocking toxin, major research efforts have focused on its catalytic domain (catBoNT/A) to design inhibitors able to counter toxin-induced post-neuronal internalization. Despite intense efforts over the past 10 years, the small inhibitors developed so far are inadequate for *in vivo* treatment; thus more effective inhibitors are still urgently needed (5). Rather potent peptide-based inhibitors have been reported, but their metabolic stability may limit their efficacy in blocking BoNT/A within neurons (6–9). Several nonpeptidic compounds exhibiting submicromolar affinity have also been reported, but evaluation of their *in vivo* potency needs further improvement (10–14). The flexibility of several loops around the active site of catBoNT/A are believed to be the factor that limits inhibitor development, because of the strong entropic penalty that accompanies inhibitor binding (11, 15). Thus, alternative strategies might be necessary for developing more potent inhibitors of BoNT/A.

Covalent inhibitors could be an alternative strategy to the noncovalent ones pursued to date if a nucleophilic amino acid within the active site of catBoNT/A could be found. Looking in the active site of catBoNT/A reveals the presence of a cysteine

* This work was supported by funds from the Commissariat à l'Energie Atomique.
[S] This article contains supplemental Table S1 and Figs. S1–S5.
The atomic coordinates and structure factors (codes 4EJ5, 4EL4, and 4ELC) have been deposited in the Protein Data Bank, Research Collaboratory for Structural Bioinformatics, Rutgers University, New Brunswick, NJ (http://www.rcsb.org/).
[1] To whom correspondence should be addressed: Commissariat à l'Energie Atomique, iBiTec-S, Service d'Ingénierie Moléculaire de Protéines, CE-Saclay, Bât. 152, 91191 Gif/Yvette, Cedex, France. Tel.: 33-1-69089565; Fax: 33-1-69089071; E-mail: vincent.dive@cea.fr.

[2] The abbreviations used are: BoNT/A, *C. botulinum* neurotoxin type A; catBoNT/A, catalytic domain of BoNT/A; MTSEA, (2-aminoethyl) methanethiosulfonate; MTSPA, 3-aminopropyl methanethiosulfonate hydrobromide; MPEG, mono-methyl PEG; Bicine, *N*,*N*-bis(2-hydroxyethyl)glycine.

residue (Cys^{165}) located near the catalytic zinc ion (see Fig. 1). Nucleophilic residues involved in catalysis have been successfully targeted by active site irreversible inhibitors, leading to the development of potent inhibitors for serine and cysteine proteases (16). Such inhibitors contain in their structure reactive electrophilic moieties selected for covalent modification of these nucleophilic residues. Targeting noncatalytic nucleophiles present in enzyme cavities is a variation of the same strategy that can been used to develop irreversible "targeted covalent inhibitors" (17). A large variety of electrophilic groups have been proposed, and some of them have been validated for *in vivo* applications, leading to irreversible inhibitors with potential therapeutic values for a variety of indications (18). Recently, acrylonitrile compounds were reported to inhibit catBoNT/A through covalent modification of Cys^{165}, but no direct proof of this modification was provided (19). This result and the above considerations led us to check whether Cys^{165} in catBoNT/A can be the target of covalent inhibitors and evaluate its potential functional role in enzyme catalysis.

EXPERIMENTAL PROCEDURES

Expression and Purification of BoNT/A Catalytic Domain—A gene encoding the catalytic domain of the BoNT/A (Met^1–Phe^{425}) was obtained from the Pasteur Institute (Dr. M. Popoff, Pasteur Institute, Paris, France). This gene was inserted into the pET28a+ vector (Novagen), between the NdeI and SalI site, generating a thrombin cleavable N-terminal His_6 affinity tag. The C134S mutant was produced from 5′-gttattgatactaattctAttaatgtgatacaaccagatgg-3′and 5′-caataactatgattaaGataattacactatgttggtctacc-3′ oligonucleotides, and C165S was produced from 5′-cagctgatattatacagtttgaatCtaaaagctttggacatgaagtttt-3′ and 5′-aaaacttcatgtccaaagcttttaGattcaaactgta taatatcagctg-3′ using a site-directed mutagenesis kit (QuikChange II). All plasmids were propagated in the *Escherichia coli* strain XL1-Blue at 37 °C, and all constructions were verified by DNA sequencing using the ABI PRISM 310 Genetic analyzer (Applied Biosystems). Recombinant proteins were expressed in *E. coli* BL21 (DE3 star) cells carrying the BoNT/A catalytic domain-encoding plasmids. C134S/C165S double mutant was produced with the same procedure, introducing the C165S mutation on the C134S mutant.

E. coli BL-21 (DE3) containing BoNT/A expression plasmids were grown overnight in Luria Broth agar (LB) with 50 μg/ml kanamycin. The cells were inoculated into fresh LB medium containing antibiotic, grown at 28 °C for 4 h at 175 rpm at an $A_{600\,nm}$ level of 0.6, Protein expression was induced by the addition of 1 mM isopropyl β-thiogalactopyranodide and then cell-cultured at 175 rpm overnight at 16 °C. The cells were grown in 2 or 4 liters of LB, and teh harvested cells were then passed through a cell disruption system at 4 °C (Constant Systems Ltd., Daventry Northants, UK) in 40 ml of ice-cold buffer A (10 mM imidazole, 500 mM NaCl, and 20 mM Tris-HCl, pH 7.9) for 1 liter of the culture containing PMSF, benzonase, 10 mM $MgCl_2$, and 10 mg/ml lysozyme. The lysate was clarified by centrifugation at 18,000 rpm for 45 min at 4 °C and subsequently passed through a 0.22-μm filter. The filtered lysate was loaded onto a 5-ml column of His Trap HP that had been equilibrated with 25 ml of buffer A. The column was washed with 10% buffer B (500 mM imidazole, 500 mM NaCl, and 20 mM Tris-HCl, pH 7.9) and eluted with 50% buffer B. The peak fractions were pooled and dialyzed overnight in 5 liters of buffer (10 mM Tris-HCl, 20 mM NaCl, pH 7.8) and clarified by centrifugation at 18,000 rpm for 30 min at 4 °C. With the solution dialyzed, proteins were loaded onto a 5-ml column His Trap Q that equilibrated with buffer C (10 mM Tris-HCl, 20 mM NaCl, pH 7.8) and eluted with a linear gradient of 0.02–1 M NaCl. Fractions of 2 ml were analyzed by 12% SDS-PAGE. Purified proteins were aliquoted and then stored at −80 °C. Purified proteins were aliquoted and then stored at −80 °C. Full form of protein containing the His tag and the thrombin cleavage was observed to display better activity when conserved at 4 °C than protein form in which the His tag was removed by thrombin cleavage; we thus decided to perform all studies with His tag-containing proteins.

Enzyme Kinetics—Enzyme catalytic efficiency assays were performed in in 40 mM HEPES, pH 7.4, at 37 °C. Substrate concentration (Mca-S-N-K-T-R-I-D-E-A-N-Q-R-A-T-K-Nle-Dap(Dnp)-NH_2) was determined by amino acid analysis. Substrate was prepared as 10 mM stock solution in dimethyl sulfoxide. Enzyme concentration was determined spectrophotometrically using $\epsilon_{280\,nm}$ = 43,527 M^{-1} cm^{-1}. Individual kinetic parameters k_{cat} and K_m were obtained from analysis of fluorescence progress curves, under steady-state rate conditions, over 0.2–5 K_m substrate concentration ranges. The experiments were carried out in black 96-well plates (non-binding-surface plates 3650; Corning Costar). Progress curves were monitored by following the increase in fluorescence at 405 nm (λ_{ex} = 320 nm), induced by the cleavage of the synthetic substrate by BoNT/A enzyme, using a photon counter spectrophotometer (Fluoroskan Ascent; Thermo-Labsystems). K_m and k_{cat} values were determined by progress curves fitting using the DYNAFIT Program (20).

Enzyme Inhibition—The rate of irreversible inhibition of BoNT/A by MTSEA and MTSPA was followed by withdrawing samples for assay at several time intervals after the mixing of enzyme and inhibitor (HEPES buffer 40 mM at pH7, 37 °C), with [I] ≫ to enzyme concentration. A plot in logarithm of residual activity against time gives the observed rate of inactivation k_{obs} using the Equation 1. Assuming that the inactivation proceeds by the rapid formation of the noncovalent enzyme-inhibitor complex, followed by a slower step leading to covalent enzyme modification, the Kitz and Wilson equation was used in its linearized form (Equation 2) to deduce K_i and k_{inact} values (21). Enzyme assays were performed as described for enzyme kinetic studies.

$$\ln(\text{residual. act}) = -k_{obs}t \quad \text{(Eq. 1)}$$

$$1/(k_{obs}) = (K_i/k_{inact})*1/[I] + 1/(k_{inact}) \quad \text{(Eq. 2)}$$

Cleavage of SNAP-25—Cleavage of recombinant full-length human SNAP-25 (isoform B, 206 amino acids, 23 kDa from Abcam, reference number ab74529) (5 μM) was initiated by adding BoNT/A or serine mutants (5 or 10 nM) in 40 mM HEPES, pH 7.4, at 37 °C. After 1 h, the reaction was stopped by adding 1 μl of TFA 50% water and SDS-PAGE sample buffer. The products were resolved by 12% SDS-PAGE gel, and protein bands were revealed by silver staining. The extent of SNAP-25

cleavage was determined by densitometric scanning of the band corresponding to the product (ImageJ program).

CD Spectroscopy—CD spectra were recorded at 25 °C on a JACSO J-810 spectropolarimeter equipped with a Peltier type temperature controlled system. The proteins were equilibrated in 10 mM sodium phosphate buffer, pH 7.5. UV spectra were recorded to compare CD spectra of wild type and mutants at similar protein concentrations (5 and 15 μM for far-UV and near-UV region, respectively) (supplemental Fig. S1 and S2). The samples were prepared exchanging conservation buffer by 10 mM sodium phosphate buffer, pH 7.5, with PD-spin trap G-25 and diluting the sample in sodium phosphate buffer until the desired protein concentration was obtained. Thermal denaturation was performed by monitoring the CD signal at 222 nm from 20 to 60 °C.

MTSEA and MTSPA Adduct Formation by Mass Spectrometry Analysis—1 ml of a solution containing BoNT/A and 32 mM MTSEA or MTSPA (40 mM HEPES buffer at pH 7, 37 °C) was diluted in 19 ml of a 50 mM ammonium bicarbonate solution, to which was added 0.6 ml of trypsin at 400 ng/ml. The samples were heated at 50 °C for 2 h. 2 μl of TFA were added to stop the enzymatic reaction. The resulting digest (0.5 μl) was manually spotted on MALDI plate with an equal volume of *R*-cyano-4-hydroxycinnamic acid matrix solution prepared at 10 mg/ml in H_2O/CH_3CN/TFA (50/50/0.4). MS spectra were recorded from crystallized samples. The DataExplorer software (4.9) from ABI was used to generate ASCII peak lists from peptide mass fingerprinting MS analyses. Each peak list was manually applied for searches using MASCOT software in the NCBInr database updated in December 2008. The parameters used for the search were as follows: a taxonomy restriction was placed to *Homo sapiens* (human), one missed trypsin cleavage was allowed, a maximum mass tolerance was set at 20 ppm because of an internal calibration made on fragments resulting from trypsin autolysis for all MS analyses and methionine oxidation was set as a variable modification. MASCOT protein Mowse scores greater than 66 (assuming $p < 0.05$) were considered significant.

Crystallization—The crystallization of the catalytic domain of neurotoxin wild type BoNT/A and C134S/C165S double mutant were screened under sitting drop vapor diffusion using ChemCryst Plates (Hampton Research) with a limited number of conditions from the "Stura" screens (22) (Molecular Dimensions) with a protein solution consisting of 7.8 mg/ml in 10 mM Tris-HCl, 150 mM NaCl, pH 7.8, for the Ser^{134}/Ser^{165} double mutant and 2.88 mg/ml in 0.01 M Tris-HCl, 0.15 M NaCl, pH 7.8, for the wild type at 20 °C in a cooled incubator. Good results were obtained under different PEG conditions and various pH. The crystal optimization strategy was to use a working condition (methodology described in Ref. 23) consisting of 36% mono-methyl PEG 2000 (MPEG-2K), 50 mM Li_2SO_4, to which various buffers at different pH were applied. Optimized conditions consisted of 80% working solution with 100 mM imidazole HCl, pH 6.0, in the reservoir. Drops consisted of 1 μl of protein solution, to which 1 μl of reservoir solution was added. Seed crystals were added with a capillary-syringe combination to the drop and allowed to grow (methodology described in Ref. 24). For flash cooling 18% MPEG-2K, 22% MPD, 10% Me_2SO, 50 mM Bicine, pH 7.5, was used as the cryoprotectant. After a short solvent exchange step, the crystals were cryo-cooled in liquid ethane. The purified MTSEA-modified catalytic domain of C134S mutant of catBoNT/A was at 3.0 mg/ml in 10 mM Tris-HCl, pH 7.9, 50 mM Li_2SO_4. Crystallization of the MTSEA-modified protein was more complicated; thus larger 3-μl drops were used as well as two separate working solutions for the addition to the protein drop and for use in the reservoir. This was part of the strategy to achieve a higher degree of protein concentration by vapor diffusion. Thus, 3 μl of 24% MPEG-550, 50 mM Li_2SO_4, imidazole malate, pH 5.5, was added to the protein drop, which was then equilibrated with a reservoir consisting of 42% PEG MPEG-550, 100 mM Li_2SO_4, 200 mM imidazole malate, pH 5.5. Seeding was used as for the double mutant. For flash cooling, the same cryoprotectant was used, but after a short solvent exchange step, the crystals were cryo-cooled in liquid nitrogen. Crystallization details are summarized briefly in supplemental Table S1.

Data Collection and Crystal Structure Determination—The cryo-cooled crystals were transported to the European Synchrotron Radiation Facility in Grenoble in accordance with the safety requirements of the Agence Française de Sécurité Sanitaire des Produits de Santé. Data for cystals of the catalytic domain of neurotoxin BoNT/A and C134S/C165S double mutant were collected on Beamline ID14-4 at 100 K from single crystals to 1.87 and 1.2 Å resolution, respectively. The crystal was found to belong to the space group $P2_1$ with cell parameters 49.3, 66.3, and 64.9 Å; $\beta = 99.1°$ (supplemental Table S1). For the MTSEA-modified single mutant, data were collected on the same beamline at a later date. The crystals also belong to the tetragonal space group $P4_32_12$ with cell parameters $a = b =$ 65.3 Å, $c = 200.9$ Å diffracting to 1.8 Å resolution. In both cases there is only one molecule in the asymmetric unit. The data were processed using MOSFLM (25) and reduced using programs from the CCP4 suite of programs. Molecular replacement was carried out with MOLREP (26) using as the model an inhibitor complex of the same protein with similar crystal parameters (Protein Data Bank code 2ILP (11)) as the starting model. After restrained refinement using Refmac (27), the amino acid differences between the two loops were corrected according to the sequence. Density fitting and refinement were carried out with the aid of electron density maps (omit σA-weighted $2F_o - F_c$ and $F_o - F_c$) calculated and displayed using the XtalView suite of programs (28) and COOT (Emsley, #42). Stereochemical analysis of the final refined model was checked with the validation tools in COOT. The waters were checked with phenix.refine (29). The refinement statistics are detailed in supplemental Table S1. The figures were made with PyMOL from DeLano Scientific LLC (PyMOL Molecular Graphics System, DeLano Scientific, San Carlos, CA).

Protein Data Bank Accession Numbers—The coordinates and structure factors for the catalytic domain of neurotoxin BoNT/A C134S/C165S double mutant and single mutant C134S-MTSEA covalent adduct have been deposited in the RCSB Protein Data Bank with the following codes: 4EJ5, 4EL4, and 4ELC, respectively.

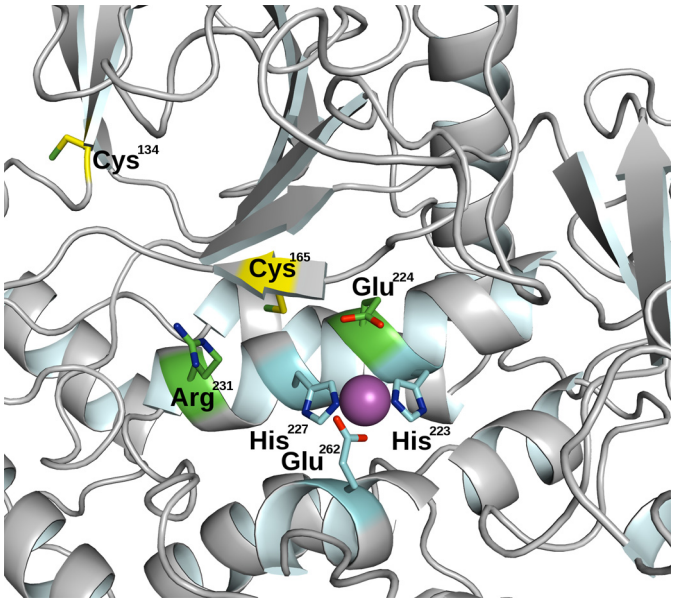

FIGURE 1. **Details of the active site of the catalytic domain of BoNT/A.** Residues chelating the zinc ion are displayed in *cyan*, residues reported to play a role in enzyme catalytic efficiency are displayed in *green*, cysteine residues are in *yellow*, and the catalytic zinc ion is shown as a *purple sphere*.

RESULTS

Functional Role of Cys^{165} in catBoNT/A—To assess the potential functional role of Cys^{165}, we expressed a recombinant version of the wild type and serine-substituted catBoNT/A. This catalytic domain possesses two free cysteines: one close to the catalytic zinc ion (Cys^{165}) and the other (Cys^{134}) far away from the active site (Fig. 1). Cys^{134} is located inside an exosite involved in the binding of SNAP-25, the natural protein substrate of BoNT/A. Impact of the replacement of these cysteine residues by serine was first evaluated by comparing the efficiency of wild type enzyme and single serine mutants to cleave SNAP-25 protein at 5 and 10 nM (see "Experimental Procedures"). As compared with wild type enzyme under the same conditions, the serine mutants performed clearly worse (Table 1 and supplemental Fig. S1). To obtain more quantitative data, the catalytic efficiency of wild type and mutant enzymes was assessed with a synthetic fluorogenic peptidic substrate. Both the wild type and the C134S mutant displayed similar catalytic efficiencies (k_{cat}/K_m) in cleaving the synthetic substrate (Table 2). This is in agreement with the fact that this synthetic substrate is much more shorter than SNAP-25; thus, its binding to catBoNT/A does not involve the exosite containing Cys^{134} (19). In contrast, a 50-fold reduction in catalytic efficiency was observed for the C165S mutant relative to the wild type. This substantial reduction in activity can be imputed to a marked decrease in k_{cat} value (0.007 s^{-1}), when compared with the wild type enzyme ($k_{cat} = 0.43\ s^{-1}$). Similar values were obtained for the C134S/C165S double mutant (Table 2).

The above data suggest that Cys^{165} plays a key role in the catalytic efficiency of catBoNT/A when cleaving both natural and synthetic substrates. To gain more insights into these findings, x-ray structures of the wild type and the C134S/C165S double mutant were determined at 1.8 and 1.2 Å, respectively.

TABLE 1

Percentage of SNAP-25 cleavage by wild type catBoNT/A catalytic domain and serine mutants

The experiments were performed in 40 mM Hepes buffer, pH 7.4, at 37 °C.

	SNAP-25 cleavage	
	5 nM of catBoNT/A	10 nM of catBoNT/A
	%	
Wild type	50	80
C134S	10	60
C165S	<10	20

TABLE 2

Kinetic parameters for the cleavage of the fluorogenic substrate (5 μM) by wild type catBoNT/A catalytic domain, C134S mutant, and C165S mutant (20 nM)

The assays were carried out in 40 mM Hepes, pH 7.4, at 37 °C.

Enzyme	K_m	k_{cat}	k_{cat}/K_m
	10^{-6} M	s^{-1}	$M^{-1}\cdot s^{-1}$
Wild type	68 ± 13	0,54 ± 0,07	7948
C134S	85 ± 11	0,54 ± 0,05	6430
C165S	76 ± 15	0,014 ± 0,001	190
C134S/C165S	35 ± 7	0,007 ± 0,008	220

Overlay of both structures shows no significant change at the active site or the exosite (Fig. 2). Consistently, CD spectra recorded in the near and far UV regions for the wild type enzyme and the mutants were similar (supplemental Figs. S2 and S3). The thermal stability was also probed by monitoring changes in ellipticity at 222 nm as a function of temperature to assess the thermal denaturation pattern. All of the proteins exhibited similar single sigmoidal transitions with identical slopes, with a midpoint of thermal transition T_m equal to 42 °C (supplemental Fig. S4). Taken together, these structural data revealed that the mutation of Cys^{165} did not induce detectable changes in the enzyme structure or active site, suggesting rather a direct role of Cys^{165} in catalysis.

Implication for Inhibitor Design—The crystal structure of BoNT/A shows that the side chain of Cys^{165} is poorly accessible to solvent (Fig. 1), thus potentially limiting its ability to be covalently modified by electrophiles. To test this, the C134S mutant, which still contains a cysteine at position 165, was incubated with MTSEA. MTSEA was selected because it contains a highly reactive sulfonyl moiety and displays a high reactivity and selectivity toward cysteine (30) (Scheme 1).

After incubation catBoNT/A with MTSEA, the enzyme activity was drastically reduced. Exhaustive dialysis did not rescue enzyme activity, suggesting that the enzyme has been irreversibly inactivated through covalent modification of Cys^{165}. A similar experiment with the C165S mutant revealed no inhibition, supporting this proposal. Monitoring the time-dependent loss of catBoNT/A when incubated in presence of different MTSEA concentrations for various time allows to determine the rate of inactivation k_{obs} as a function of MTSEA concentrations (see "Experimental Procedures"). From these data, using Equation 2, the kinetic parameters for the inactivation of catBoNT/A by MTSEA can be derived (Fig. 3 and Table 3). After trypsin digestion of the C134S mutant preincubated with MTSEA, mass spectrometry analysis of the resulting peptides revealed a mass increment of 74 Da for the fragment of catBoNT/A containing Cys^{165}, which is consistent with a Cys-MTSEA disulfide adduct (supplemental Fig. S5*A*). The x-ray

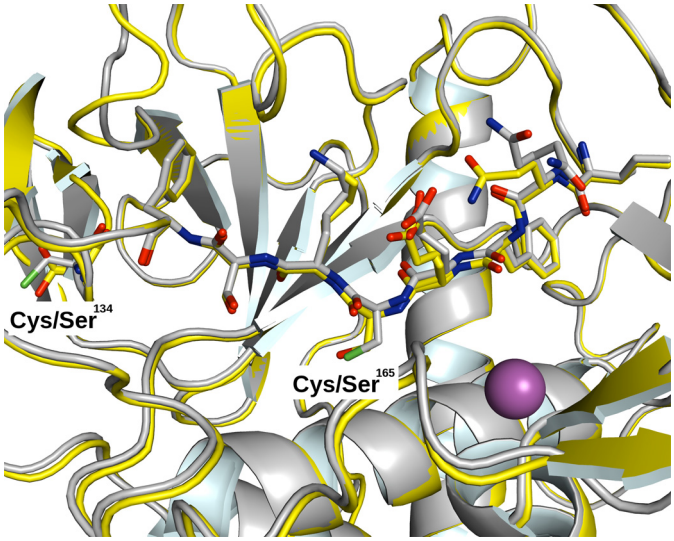

FIGURE 2. **Superimposition of crystal structure between wild type catBoNT/A catalytic domain (1. 8 Å) and C134S/C165S double mutant (1.2 Å).** A closer view of the peptide segment bearing Cys^{165} in wild type (*yellow*) or C134S/C165S in double mutant (*cyan*) is shown in stick representation.

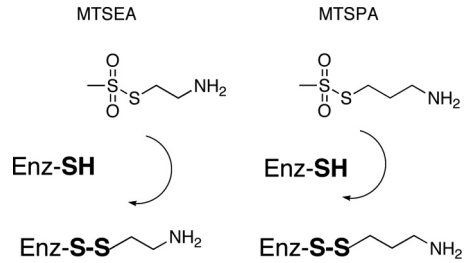

SCHEME 1. **Chemical structure of MTSEA and MTSPA compounds and chemical reaction with cysteine.**

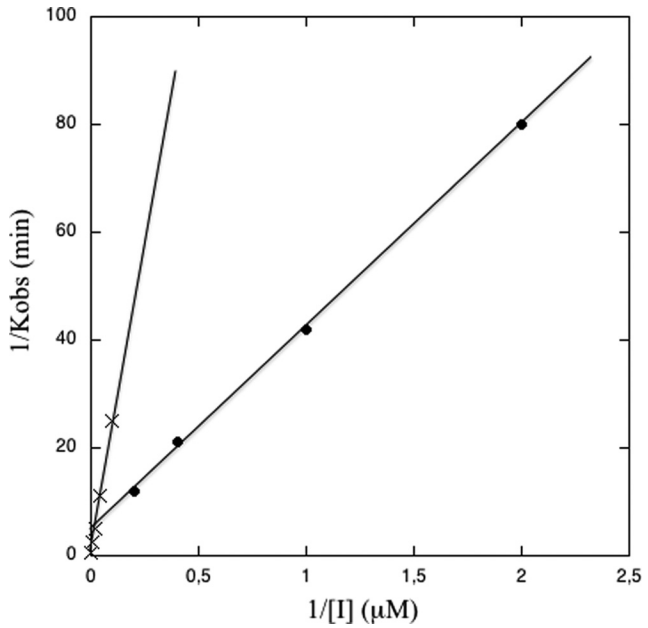

FIGURE 3. **Kitz-Wilson plot for the inactivation of catBoNT/A by MTSEA (*cross*) and by MTSPA (*closed circle*).** 40 mM HEPES buffer at pH 7 at 37 °C was used.

structure of the C134S mutant modified with MTSEA determined at 1.72 Å resolution confirms this finding. Interestingly, this structure revealed that the amino group of MTSEA was

TABLE 3
Kinetic constant for the inactivation of catBoNT/A catalytic domain by MTSEA and MTSPA

The experiments were performed in 40 mM Hepes, pH 7.4, at 37 °C, and the kinetic constants were determined from plots reported in Fig. 3.

Inhibitor	k_{inact}	K_i	k_{inact}/K_i
	s^{-1}	μM	$M^{-1}\cdot s^{-1}$
MTSEA	0.041	625	65
MTSPA	0.0034	7.7	440

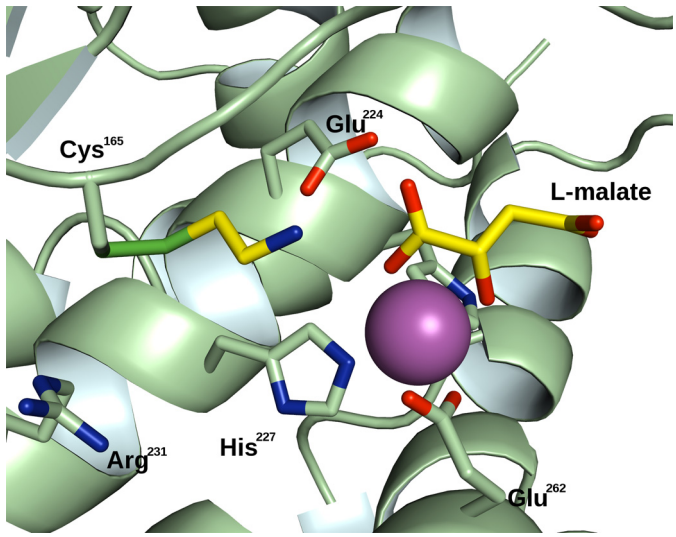

FIGURE 4. **Crystal structure of catBoNT/covalently modified by MTSEA.** This structure reveals the NH_3 group of MTSEA is surrounded by Glu^{224}, the zinc ion, and a malate molecule from the crystallization buffer, interacting itself with the zinc ion.

pointing toward Glu^{224} and that a malate molecule from the crystallization buffer was chelating the zinc ion (Fig. 4). From this structure, we speculated that the longer MTSPA compound (Scheme 1) with an additional methylene might increase inhibitor potency by allowing its NH_2 group to better interact with Glu^{224} or the zinc ion. MTSPA was also found to irreversibly inhibit catBoNT/A (Fig. 3), and kinetic analyses confirmed that MTSPA is a better inhibitor than MTSEA (Table 3), mostly because of the increase in affinity (MTSPA, K_i value of 7.7 μM; MTSEA, K_i = 625 μM). MTSPA is a rather potent of BoNT/A, because after 2 h of incubation, it displays an IC_{50} value of 260 nM. Mass spectrometry analyses confirmed that MTSPA covalently modified Cys^{165} (supplemental Fig. S5*B*). Similar results were also obtained with the wild type enzyme, with the two compounds displaying IC_{50} values comparable with those obtained for the C134S mutant.

Metallopeptidases with Cysteine Residue in Their Active Site—Systematic analysis of the Protein Data Bank revealed that other zinc proteases likewise have a cysteine in a similar position to BoNT/A in their active sites. In the majority of zinc peptidases, a HE*XX*H signature is found in which the two histidines bind the active site metal ion and the glutamate acts as the general base/acid during catalysis. These key active site residues were used to perform the superimposition of available three-dimensional structures (Fig. 5). Of the seven proteases identified in the Protein Data Bank, six contained a zinc ion in their active sites and one contained a cobalt. The superposition confirmed not only the presence but also the topological equivalence of the

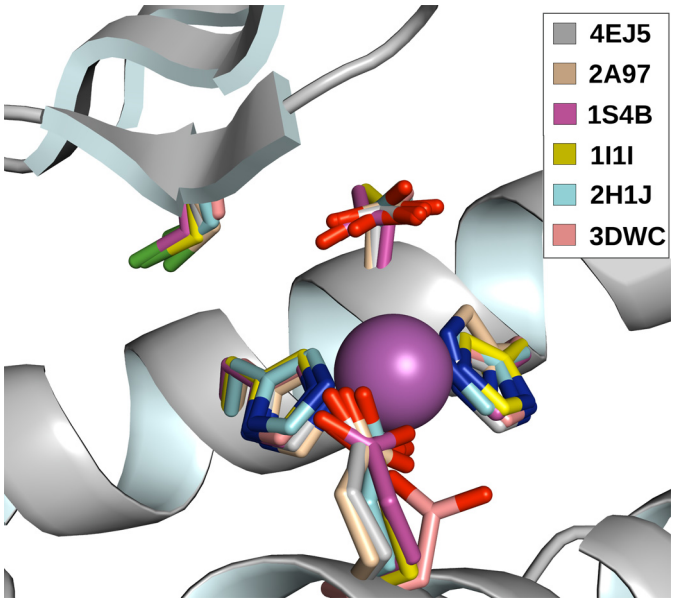

FIGURE 5. **Superimposition of the crystal structure of *C. botulinum* neurotoxin type A (Protein Data Bank code 1XTG) with that of *C. botulinum* neurotoxin type F (Protein Data Bank code 2A97), thimet oligopeptidase (Protein Data Bank code 1S4B), neurolysin (Protein Data Bank code 1I1I), oligopeptidase F (Protein Data Bank code 2H1J), and *T. cruzi* metallocarboxypeptidase (Protein Data Bank code 3DWC).** The structure overlay was based on the best fit between the zinc ligand (His, His, and Glu) in these proteases.

cysteine site in all these structures, thus pointing to a common functional role. These peptidases are expressed by different kingdoms of life: eukaryotes with mammalian thimet oligopeptidase (Protein Data Bank code 1S4B) and neurolysin (Protein Data Bank code 1I1I); prokaryotes (*C. botulinum* neurotoxins type A (Protein Data Bank code 1XTG) and type F (Protein Data Bank code 2A97) and oligopeptidase F (Protein Data Bank code 2H1J) from *Bacillus stearothermophilus*); and protists (*Trypanosoma cruzi* metallocarboxypeptidase (Protein Data Bank code 3DWC)). All of these metallopeptidases belong to the "cowrin family" according to the proposed nomenclature of Gomis-Ruth (31). However, not all members of the cowrin family possess this cysteine residue. For example, in mammalian angiotensin-concerting enzyme, structurally related to thimet oligopeptidase and neurolysin, a serine is observed at the topological equivalent position to the cysteine and in *T. thermophilus* carboxypeptidase (Protein Data Bank code 1WGZ), closely related to *T. cruzi* metallocarboxypeptidase (32), a glutamate residue is observed at this site.

DISCUSSION

The presence of a cysteine close to the active site metal ion in a subset of metallopeptidases whose side chain is not pointing toward the solvent from crystal structure is intriguing. The present study reveals that in catBoNT/A Cys^{165} is not playing a key structural role but contributes to in enzyme activity. The 50-fold reduction in catalytic efficiency of the C165S mutant in cleaving a synthetic substrate is comparable with that reported for other mutants of catBoNT/A, Arg^{231} (33), Arg^{362}, and Tyr^{365} (34), three residues involved in the stabilization of the transition state. These mutations rendered a reduction in k_{cat} (65-fold for Arg → Ala^{231}, 84-fold for Arg → Ala^{363}, and 35-fold for Tyr → Phe^{365}) close to the 60-fold reduction in k_{cat} observed for the C165S mutant of catBoNT/A. This mutation also greatly affects the cleavage of a natural substrate, suggesting a functional relevance for this result. Combining experimental approaches, we conclude that the effect of the Cys^{165} → Ser mutation on enzyme activity does not result from structural perturbations but rather from the suppression of sulfur chemistry. Without information on the structure of reaction intermediates involved in substrate cleavage, the precise role of Cys^{165} in enzyme activity is difficult to assess. However, it should be kept in mind that a cysteine residue, particularly one located at the protein surface like Cys^{165}, is highly polarizable and carries a terminal dipole with a pronounced partial negative charge. These are properties that render cysteine able to perform multiple interactions and to change its reactivity when the local pH is altered within its microenvironment (35). In this respect, the short distance between Cys^{165} and Arg^{231} (Cys^{165} Sg to Arg^{231} Ne, 4.9 Å), a residue involved in enzyme catalysis, may suggest a possible concerted action between these two residues during catalysis. To further assess the functional role of Cys^{165}, we retrieved all sequences for serotype A and F orthologues found in different clostridial strains to assess conservation. For BoNT/A, all 18 sequences identified contained the cysteine, whereas only 6 of 16 BoNT/F sequences exhibited a cysteine (supplemental Fig. S5). Obviously, better understanding the exact role of Cys^{165} in enzyme catalysis will require additional studies.

From crystal structure of catBoNT/A, the reduced accessibility of the Cys^{165} sulfur atom could have limited its covalent modification by electrophilic groups. The successful covalent modification of Cys^{165} thus suggests the existence of some local "flexibility" permitting the sulfonate reactive group of MTSEA and MTSPA to reach and react with the Cys^{165} thiol group. The present work also supports the covalent modification of Cys^{165} by acrylonitrile as recently speculated (19). The most potent inhibitor of catBoNT/A reported to date is a pseudoheptapeptide, which exhibits a K_i value of 41 nM (7); in addition, many low molecular weight inhibitors have been reported to evince submicromolar potency (5). Instead of increasing the size of the noncovalent inhibitors to further optimize interactions with enzyme active site, the present study reveals on a structural basis how small covalent inhibitors of catBoNT/A can be developed. To design irreversible inhibitors, the availability of detailed structural information is critical for positioning the electrophilic moiety of the inhibitor correctly, so that it can attack the nucleophile present in the enzyme active site efficiently and yield the desired covalent modification. Compared with noncovalent inhibitors, the potency and selectivity of irreversible inhibitors can be optimized in two ways: by modulating the binding capacity of the nonreactive part of the inhibitor and by modifying the reaction rate between the nucleophile and the electrophile. When properly designed, irreversible inhibitors can be exceptionally potent and selective because part of the binding energy is derived from the protein-inhibitor covalent bond (17, 36). Thus, in a context where programs based on noncovalent inhibitor development have been disappointing, development of covalent inhibitors may represent a new avenue. The crystal structure of BoNT/A-MTSEA complex is a

very good starting point for designing libraries of small compounds, containing on one side various electrophilic groups and on the other different zinc-chelating groups. In this structure, an L-malic acid molecule is making interactions with the amino group of MTSEA, the zinc ion and residues Glu^{224} and Tyr^{366}. From these observations, inhibitors can also be designed by "connecting" the L-malic acid to electrophiles, a classical approach in fragment-based design (37). Using similar structure-based design, a very potent covalent inhibitor of HCV protease has been recently reported (38). For the purpose of this study, we have selected as electrophile a sulfonyl group, which is too reactive in context of complex proteome or cell systems; thus in the future less reactive electrophiles like acrylonitrile would have to be chosen for developing useful covalent inhibitors of BoNT/A.

Analysis of the Protein Data Bank reveals that other zinc peptidases likewise exhibit a cysteine in their active sites and that the topology of these cysteine residues is very well conserved (Fig. 5). Although in catBoNT/A, Cys^{165} is close to Arg^{230}, a structural context that may influence the reactivity or function of Cys^{165}, in other analyzed proteins there is not an arginine equivalent that would lead to a modulated cysteine reactivity. Whether the conserved cysteines in these proteases are also involved in enzyme catalysis needs to be clarified. Whatever the exact roles of these cysteines are, their use to develop targeted covalent inhibitors for these will only depend on their reactivity and flexibility. Among the most interesting potential targets are a family of zinc carboxypeptidases expressed by pathogens like *Vibrio cholerae*, *Yersinia pseudotuberculosis* and *peptis*, *Leismania major*, and *T. cruzi*. Thus, beyond BoNT/A inhibitors, the results reported here should stimulate the development of targeted covalent inhibitors of these carboxypeptidases.

REFERENCES

1. Oguma, K., Fujinaga, Y., and Inoue, K. (1995) Structure and function of *Clostridium botulinum* toxins. *Microbiol. Immunol.* **39,** 161–168
2. Willis, B., Eubanks, L. M., Dickerson, T. J., and Janda, K. D. (2008) The strange case of the botulinum neurotoxin. Using chemistry and biology to modulate the most deadly poison. *Angew Chem. Int. Ed. Engl.* **47,** 8360–8379
3. Arnon, S. S., Schechter, R., Inglesby, T. V., Henderson, D. A., Bartlett, J. G., Ascher, M. S., Eitzen, E., Fine, A. D., Hauer, J., Layton, M., Lillibridge, S., Osterholm, M. T., O'Toole, T., Parker, G., Perl, T. M., Russell, P. K., Swerdlow, D. L., and Tonat, K. (2001) Botulinum toxin as a biological weapon. Medical and public health management. *JAMA* **285,** 1059–1070
4. Simpson, L. L. (2004) Identification of the major steps in botulinum toxin action. *Annu. Rev. Pharmacol. Toxicol.* **44,** 167–193
5. Li, B., Peet, N. P., Butler, M. M., Burnett, J. C., Moir, D. T., and Bowlin, T. L. (2011) Small molecule inhibitors as countermeasures for botulinum neurotoxin intoxication. *Molecules* **16,** 202–220
6. Schmidt, J. J., Stafford, R. G., and Bostian, K. A. (1998) Type A botulinum neurotoxin proteolytic activity. Development of competitive inhibitors and implications for substrate specificity at the S1′ binding subsite. *FEBS Lett.* **435,** 61–64
7. Zuniga, J. E., Schmidt, J. J., Fenn, T., Burnett, J. C., Araç, D., Gussio, R., Stafford, R. G., Badie, S. S., Bavari, S., and Brunger, A. T. (2008) A potent peptidomimetic inhibitor of botulinum neurotoxin serotype A has a very different conformation than SNAP-25 substrate. *Structure* **16,** 1588–1597
8. Kumaran, D., Rawat, R., Ahmed, S. A., and Swaminathan, S. (2008) Substrate binding mode and its implication on drug design for botulinum neurotoxin A. *PLoS Pathog.* **4,** e1000165
9. Hale, M., Oyler, G., Swaminathan, S., and Ahmed, S. A. (2011) Basic tetrapeptides as potent intracellular inhibitors of type A botulinum neurotoxin protease activity. *J. Biol. Chem.* **286,** 1802–1811
10. Burnett, J. C., Ruthel, G., Stegmann, C. M., Panchal, R. G., Nguyen, T. L., Hermone, A. R., Stafford, R. G., Lane, D. J., Kenny, T. A., McGrath, C. F., Wipf, P., Stahl, A. M., Schmidt, J. J., Gussio, R., Brunger, A. T., and Bavari, S. (2007) Inhibition of metalloprotease botulinum serotype A from a pseudo-peptide binding mode to a small molecule that is active in primary neurons. *J. Biol. Chem.* **282,** 5004–5014
11. Silvaggi, N. R., Boldt, G. E., Hixon, M. S., Kennedy, J. P., Tzipori, S., Janda, K. D., and Allen, K. N. (2007) Structures of *Clostridium botulinum* neurotoxin serotype A light chain complexed with small-molecule inhibitors highlight active-site flexibility. *Chem Biol.* **14,** 533–542
12. Moe, S. T., Thompson, A. B., Smith, G. M., Fredenburg, R. A., Stein, R. L., and Jacobson, A. R. (2009) Botulinum neurotoxin serotype A inhibitors. Small-molecule mercaptoacetamide analogs. *Bioorg Med. Chem.* **17,** 3072–3079
13. Burnett, J. C., Wang, C., Nuss, J. E., Nguyen, T. L., Hermone, A. R., Schmidt, J. J., Gussio, R., Wipf, P., and Bavari, S. (2009) Pharmacophore-guided lead optimization. The rational design of a non-zinc coordinating, sub-micromolar inhibitor of the botulinum neurotoxin serotype a metalloprotease. *Bioorg Med. Chem. Lett.* **19,** 5811–5813
14. Li, B., Pai, R., Cardinale, S. C., Butler, M. M., Peet, N. P., Moir, D. T., Bavari, S., and Bowlin, T. L. (2010) Synthesis and biological evaluation of botulinum neurotoxin a protease inhibitors. *J. Med. Chem.* **53,** 2264–2276
15. Breidenbach, M. A., and Brunger, A. T. (2004) Substrate recognition strategy for botulinum neurotoxin serotype A. *Nature* **432,** 925–929
16. Powers, J. C., Asgian, J. L., Ekici, O. D., and James, K. E. (2002) Irreversible inhibitors of serine, cysteine, and threonine proteases. *Chem. Rev.* **102,** 4639–4750
17. Singh, J., Petter, R. C., Baillie, T. A., and Whitty, A. The resurgence of covalent drugs. *Nat. Rev. Drug Discov.* **10,** 307–317
18. Potashman, M. H., and Duggan, M. E. (2009) Covalent modifiers. An orthogonal approach to drug design. *J. Med. Chem.* **52,** 1231–1246
19. Li, B., Cardinale, S. C., Butler, M. M., Pai, R., Nuss, J. E., Peet, N. P., Bavari, S., and Bowlin, T. L. Time-dependent botulinum neurotoxin serotype A metalloprotease inhibitors. *Bioorg Med. Chem.* **19,** 7338–7348
20. Kuzmic, P. (1996) Program DYNAFIT for the analysis of enzyme kinetic data. Application to HIV proteinase. *Anal. Biochem.* **237,** 260–273
21. Kitz, R., and Wilson, I. B. (1962) Esters of methanesulfonic acid as irreversible inhibitors of acetylcholinesterase. *J. Biol. Chem.* **237,** 3245–3249
22. Stura, E. A., Nemerow, G. R., and Wilson, I. A. (1992) Strategies in the crystallization of glycoproteins and protein complexes. *J. Crystal Growth* **122,** 273–285
23. Stura, E. A. (1999) Strategy 3. Reverse Screening, in *Crystallization of Proteins: Techniques, Strategies and Tips. A Laboratory Manual* (Bergfors, T., ed) pp. 113–124, International University Line
24. Stura, E. A. (1999) Seeding, in *Crystallization of Proteins: Techniques, Strategies and Tips. A Laboratory Manual* (Bergfors, T., ed) pp. 141–153, International University Line
25. Leslie, A. G. (2006) The integration of macromolecular diffraction data. *Acta Crystallogr. D Biol. Crystallogr.* **62,** 48–57
26. Vagin, A., and Teplyakov, A. (2010) Molecular replacement with MOLREP. *Acta Crystallogr. D Biol. Crystallogr.* **66,** 22–25
27. Murshudov, G. N., Vagin, A. A., and Dodson, E. J. (1997) Refinement of macromolecular structures by the maximum-likelihood method. *Acta Crystallogr. D Biol. Crystallogr.* **53,** 240–255
28. McRee, D. E. (1999) XtalView/Xfit. A versatile program for manipulating atomic coordinates and electron density. *J. Struct. Biol.* **125,** 156–165
29. Adams, P. D., Afonine, P. V., Bunkoczi, G., Chen, V. B., Davis, I. W., Echols, N., Headd, J. J., Hung, L. W., Kapral, G. J., Grosse-Kunstleve, R. W., McCoy, A. J., Moriarty, N. W., Oeffner, R., Read, R. J., Richardson, D. C., Richardson, J. S., Terwilliger, T. C., and Zwart, P. H. PHENIX. A comprehensive Python-based system for macromolecular structure solution. *Acta Crystallogr. D Biol. Crystallogr.* **66,** 213–221
30. Stauffer, D. A., and Karlin, A. (1994) Electrostatic potential of the acetylcholine binding sites in the nicotinic receptor probed by reactions of binding-site cysteines with charged methanethiosulfonates. *Biochemistry* **33,**

6840–6849
31. Gomis-Ruth, F. X. (2008) Structure and mechanism of metallocarboxypeptidases. *Crit. Rev. Biochem. Mol. Biol.* **43,** 319–345
32. Niemirowicz, G., Fernandez, D., Sola, M., Cazzulo, J. J., Aviles, F. X., and Gomis-Ruth, F. X. (2008) The molecular analysis of *Trypanosoma cruzi* metallocarboxypeptidase 1 provides insight into fold and substrate specificity. *Mol. Microbiol.* **70,** 853–866
33. Ahmed, S. A., Olson, M. A., Ludivico, M. L., Gilsdorf, J., and Smith, L. A. (2008) Identification of residues surrounding the active site of type A botulinum neurotoxin important for substrate recognition and catalytic activity. *Protein J.* **27,** 151–162
34. Binz, T., Bade, S., Rummel, A., Kollewe, A., and Alves, J. (2002) Arg^{362} and Tyr^{365} of the botulinum neurotoxin type a light chain are involved in transition state stabilization. *Biochemistry* **41,** 1717–1723
35. Marino, S. M., and Gladyshev, V. N. (2010) Structural analysis of cysteine *S*-nitrosylation. A modified acid-based motif and the emerging role of trans-nitrosylation. *J. Mol. Biol.* **395,** 844–859
36. Smith, A. J., Zhang, X., Leach, A. G., and Houk, K. N. (2009) Beyond picomolar affinities. Quantitative aspects of noncovalent and covalent binding of drugs to proteins. *J. Med. Chem.* **52,** 225–233
37. Rees, D. C., Congreve, M., Murray, C. W., and Carr, R. (2004) Fragment-based lead discovery. *Nat. Rev. Drug Discov.* **3,** 660–672
38. Hagel, M., Niu, D., St Martin, T., Sheets, M. P., Qiao, L., Bernard, H., Karp, R. M., Zhu, Z., Labenski, M. T., Chaturvedi, P., Nacht, M., Westlin, W. F., Petter, R. C., and Singh, J. (2011) Selective irreversible inhibition of a protease by targeting a noncatalytic cysteine. *Nat. Chem. Biol.* **7,** 22–24